

AERODYNAMIC ASPECTS OF FLAPPING WING MICRO AIR VEHICLES

J. Szmelter¹, R. Żbikowski²

¹Department of Environmental & Ordnance Systems

²Department of Aerospace, Power & Sensors

Cranfield University, RMCS Shrivenham, Swindon SN6 8LA, England, UK

Keywords: *micro air vehicles, insect-like flapping flight, CFD*

Abstract

The main objective of this paper is to discuss the nature of the little known aerodynamics of the flapping wing micro air vehicles (MAVs), inspired by insect flight. These small (ca 6 inches, or hand-held) reconnaissance vehicles will fly inside buildings, which requires hover for observation and agility at low speeds to move in confined spaces. For this flight envelope insect-like flapping flight seems to be an optimal mode of flying.

The investigation of the aerodynamics of the flapping wing MAVs is very challenging. The problem involves complex unsteady, viscous flows (dominantly laminar) with the moving wing generating vortices and interacting with them. At this early stage of research a strategy for numerical modelling has been established. The initial CFD capabilities and their application are described. In particular, scaled up wings of a *Bibio* fly are used with representative wing kinematics to analyse steady-state, inviscid flow in forward flight.

1 Introduction

The development of small (ca 6 inches, or hand-held) autonomous flying vehicles is motivated by a need for intelligent reconnaissance robots, capable of discreetly penetrating confined spaces and manoeuvring in them without the assistance of a human telepilot [13, 14].

Flying inside buildings, stairwells, shafts and

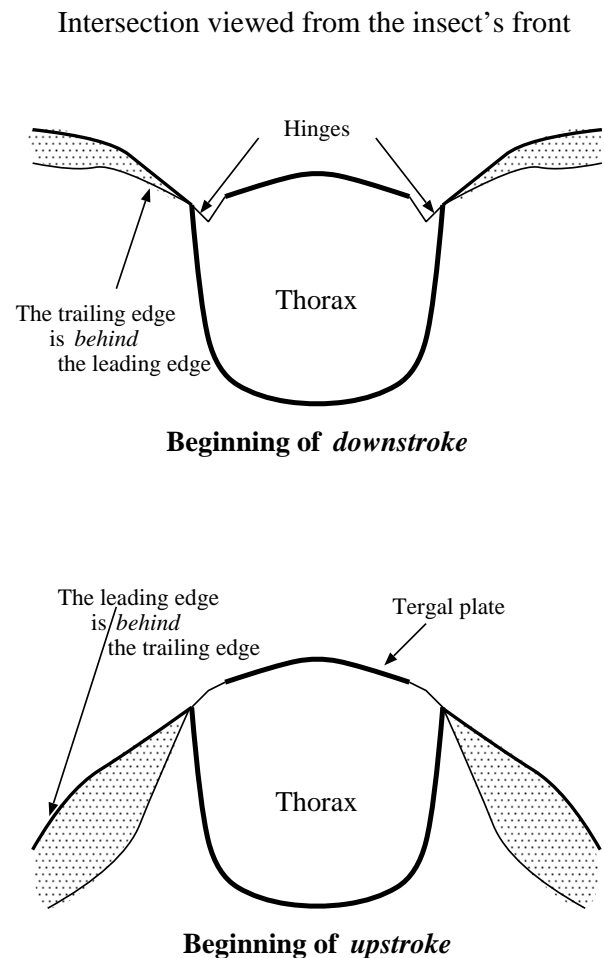


Fig. 1 Insect wing flapping

tunnels is of significant military and civilian value, and requires agility at low speeds to avoid obstacles and move in confined spaces. The vehicles can be used in dull, dirty or dangerous (D^3) environments, where direct or remote human assistance is not feasible. Non-military uses will include law enforcement and rescue operations. The ability to explore D^3 environments without human involvement will be of interest for many industries, allowing air sampling in non-attainment areas, examination of confined spaces in buildings, installations and large machines. The flight envelope of MAVs requires high agility (including hover) at low speeds (a few mph) and silent flight, which does not make scaled down fixed wing aircraft or rotorcraft attractive. Therefore, insect-like flapping flight seems to be an optimal mode of flying for highly manoeuvrable flight through confined spaces [13, 14].

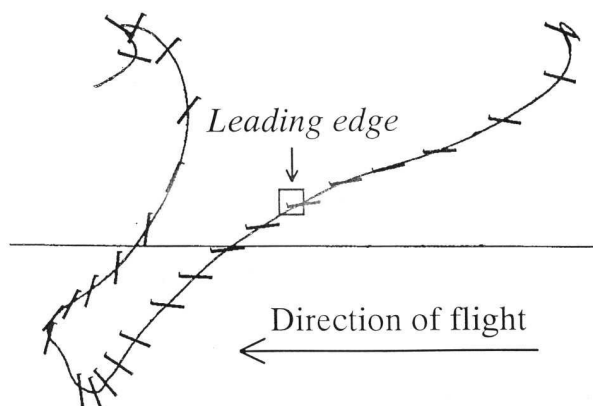


Fig. 2 Typical motions of fly's flapping wing [12, page 6].

1.1 Insect-like flapping

This unconventional aerodynamic concept deserves a more detailed explanation. Insects fly by oscillating (frequency range: 5–200 Hz) and rotating their wings through large angles, which is possible because their wing articulation is not limited by an internal skeleton. The wingbeat cycle can be divided into two phases: downstroke and upstroke (see Figures 1 and 2). At the beginning of downstroke, the wing (as seen from

the front of the insect) is in the uppermost position with the leading edge pointing forward. The wing is then pushed downwards and rotated continuously, so that the angle of attack changes considerably during this downward motion. At the end of downstroke, the wing is twisted rapidly, so that the leading edge points backwards, and the upstroke begins. During the upstroke the wing is pushed upwards and rotated again, which changes the angle of attack throughout this motion. At the highest point, the wing is twisted again, so that the leading edge points forward and the next downstroke begins. In forward flight the downstroke lasts longer than the upstroke, because of the need to generate thrust; in hover they are equal.

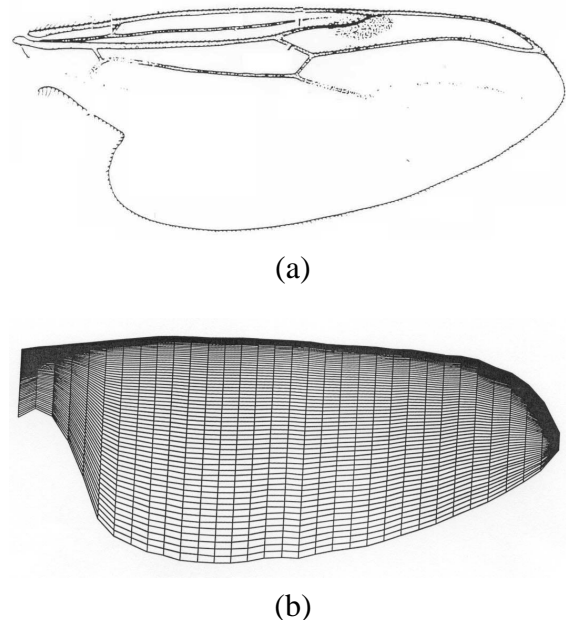


Fig. 3 Insect-like flapping wing considered: (a) fore wing of a fly of *Bibio* (Diptera: Bibionidae) [9, page 46]; (b) simplified geometry and mesh representation used in calculations.

This mode of flying relies on unsteady aerodynamics [6], producing high lift coefficients (peak C_L of the order of 3 is typical [3]) and excellent manoeuvrability. The unsteady mechanism varies with different insects; the most important mechanism is a bound leading edge vortex [7]. The high lift is a major factor in high efficiency of the scheme: a typical power requirement for insects is 30 W/kg [4],

whereas small, electrically-powered, propeller-driven, fixed wing aircraft require about 150 W/kg. Insect flapping occurs in a stroke plane that generally remains at the same orientation to the body and is either horizontal or inclined. Rapid rotations occur at each end of the flapping half-stroke. To a first approximation, kinematic control of insect flight manoeuvres is provided by changes in the tilt of the stroke plane, which is analogous to helicopter control. Precise control is achieved by including inter-wing differences in: the magnitude of force production, timing of the downstroke-to-upstroke wing rotation and the geometric position of the wings when the rotation occurs.

1.2 Our approach to flapping wing aerodynamics

The flapping wing MAV is a novel aerodynamic concept and the main long-term objective of our work is to produce design guidelines for flapping wings. These studies are undertaken with a view to their application to high performance flight control, taking inspiration from insect flight. In defining flapping wing design methodology firstly the basic constraints of the design need to be reviewed, focusing on the required wing motion and its aerodynamics, and structural and materials considerations. A detailed study of wing motion has to be complemented by flutter analysis and control implications, as required for a realistic design. In the study a decision must be made whether to keep a rigid profile or to allow for dynamic change of camber and/or twist during flapping. Main inputs to this phase will be provided by the existing entomological knowledge and from the parallel project underway at Cranfield University (RMCS Shrivenham) aimed at building a technology demonstrator of smart flapping wings.

In the next step, an initial planform shape should be proposed, taking inspiration from Nature, and has to be investigated with special emphasis on scaling effects. After the planform shape considerations, the analysis of aerofoils ought to be done, using basic aerodynamic and

geometric constraints as a starting point.

In our long-term study a preliminary assessment of the planform shape and aerofoils will be performed using modified blade element theory. Classical blade element theory has been successfully developed for analysing insect wing aerodynamics, at least for the steady-flow contribution [5]. Modifications to the classic blade element theory will be along the lines described by Adkins & Liebeck [1] for propellers. This will eliminate small angle assumptions and allow accurate calculation of vortex displacement velocity (and hence section drag). This has been shown to be very successful for propellers, but has not previously been applied to flapping wing analysis. It has the additional advantage of involving very rapid calculations. Further refinements to the blade element calculations will be made using line lifting theory.

In the investigation of aerodynamics of flapping wings the focus will be on studies showing sensitivity of the flow to the variation of wing kinematics, change in wing planform shape, aerofoils' shape and their distribution along the wing span. The effect of changes in aerofoils' thickness and camber will have to be explored, as well. In order to meet these challenges wing design will have to employ advanced CFD tools, i.e., time-accurate Navier-Stokes solvers. Although the flows observed in nature indicate that insects fly in laminar flows, for design purposes it is prudent to include turbulence modelling.

At this stage of our work, only very basic CFD capabilities have been achieved. However, they can already provide initial insight into the aerodynamic aspects of flapping wing MAVs.

2 Current CFD methodology

As explained in Section 1, the aerodynamics of the flapping wing micro air vehicles is highly non-trivial and involves unsteady, low speed, low Re , viscous flow (dominantly laminar), with an attached leading edge vortex and wing-vortex interactions. At this preliminary stage, simplifying assumptions have been introduced to allow for the initial CFD modelling. Speeds characteristic

for this problem are low and therefore the flow is treated as an incompressible fluid. For numerical simplicity the flow is also assumed to be inviscid. For such idealised fluids the continuity and Euler equations can be written as:

$$\begin{aligned} \frac{\partial u}{\partial x} + \frac{\partial v}{\partial y} + \frac{\partial w}{\partial z} &= 0 \\ \frac{\partial u}{\partial t} + u \frac{\partial u}{\partial x} + v \frac{\partial u}{\partial y} + w \frac{\partial u}{\partial z} + \frac{\partial p}{\partial x} &= 0 \\ \frac{\partial v}{\partial t} + u \frac{\partial v}{\partial x} + v \frac{\partial v}{\partial y} + w \frac{\partial v}{\partial z} + \frac{\partial p}{\partial y} &= 0 \\ \frac{\partial w}{\partial t} + u \frac{\partial w}{\partial x} + v \frac{\partial w}{\partial y} + w \frac{\partial w}{\partial z} + \frac{\partial p}{\partial z} &= 0, \end{aligned} \quad (1)$$

where p indicates pressure and u, v, w are the Cartesian velocity components in x, y, z directions.

The numerical solution is based on the three dimensional, Jameson-Runge-Kutta type [10], explicit, finite volume, cell centred code. To avoid numerical stability limitations imposed for the explicit solvers on the time step by the CFL conditions for incompressible flows the artificial compressibility approach has been employed. The method, originally proposed by Chorin [2], has been already used in the context of flapping wing modelling by Liu and Kawachi [11]. In the work presented here the developments reported in [8] have been closely followed.

The continuity equation in (1), representing the incompressibility condition, can be modified by adding the artificial compressibility term:

$$\frac{\partial p}{\partial t^*} \frac{1}{c^{*2}}, \quad (2)$$

where c^* corresponds to a finite artificial speed of sound (infinite for incompressible flows) and t^* indicates pseudo time. In this way, the mathematical character of equations (1) is changed to a system of hyperbolic equations for which an explicit flow solver can be employed.

The modified set of equations (1) can be written in the form:

$$\frac{\partial \mathbf{w}}{\partial t^*} + \Phi \left(\frac{\partial \mathbf{f}}{\partial x} + \frac{\partial \mathbf{g}}{\partial y} + \frac{\partial \mathbf{h}}{\partial z} \right) = 0, \quad (3)$$

where the vector of dependent variables \mathbf{w} and the flux vectors $\mathbf{f}, \mathbf{g}, \mathbf{h}$ are given by:

$$\begin{aligned} \mathbf{w} &= [p \quad u \quad v \quad w]^T \\ \mathbf{f} &= [u \quad u^2 + p \quad uv \quad uw]^T \\ \mathbf{g} &= [v \quad vu \quad v^2 + p \quad vw]^T \\ \mathbf{h} &= [w \quad wu \quad wv \quad w^2 + p]^T \end{aligned} \quad (4)$$

and matrix Φ can be written as:

$$\Phi = \begin{bmatrix} c^{*2} & 0 & 0 & 0 \\ 0 & 1 & 0 & 0 \\ 0 & 0 & 1 & 0 \\ 0 & 0 & 0 & 1 \end{bmatrix}. \quad (5)$$

In steady state, time derivatives reduce to zero and solutions of the systems of equations (1) and (3) become equivalent. The artificial compressibility method can be further extended (as shown for example in [11]) to treat time dependent flows. This extended method relies on introduction of time intervals. Within each interval additional iterations in pseudo time are performed and the assumption is made that the flow reaches a steady state for this interval.

In this paper we present only the steady state calculations. The currently employed CFD modelling is insufficiently mature to capture the true nature of the flow and work continues on further developments of the code. In particular, the code is being extended to include viscous terms to solve the laminar Navier-Stokes equations. To ensure good accuracy in time-dependent solution of the flow the method is being extended to incorporate the semi-implicit operator splitting approach, with the implicit part employing a conjugate gradient pressure solver.

In the presented calculations the structured single block C-H mesh is used. In a later stage the prescribed flapping movement of the wing (with possible option in the change of the wing planform) will require a dynamic remeshing technique. This can be achieved by the use of the same fast conformal mapping techniques as these applied in the generation of the initial mesh.

3 Numerical results

Sample calculations illustrating current capabilities of the method and providing a preliminary

insight into the aerodynamic behaviour of flapping wing have been performed for a low speed (7 m/s) forward flight. At this stage the choice of the wing planform, shape of aerofoils forming the wing as well as the prescribed kinematics of movement are still open questions. The aerodynamic design and thorough understanding of physics involved will be a subject of a long term detailed study. In the presented calculations the choice of the planform has been inspired by the geometry of the wing of a *Bibio* fly. The potential choice of generic geometry of the planform is illustrated in Figure 3 (a). The geometry used in calculations was simplified and the corresponding computational mesh is shown in Figure 3(b).

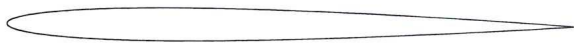


Fig. 4 Wing section profile used in calculations.

A constant aerofoil section was used along the wing span and scaled with respect to local chord to fit the planform. A symmetric NACA0012 aerofoil with thickness decreased 0.3 times was chosen as a starting point of investigation (Figure 4). It is anticipated from observation of insects that the design of final aerofoil sections will result in still much thinner aerofoils characterised by a sharp leading edge. A choice of wing positions which were investigated was dictated by a typical changes of the rotational angles around the Cartesian x, y, z axes, with x, y defining an aerofoil plane and z orientated from the root to the tip of a wing. The rotation angles were interpreted from the kinematics presented in Figure 2. It was assumed that during one cycle:

- the rotation angle γ with respect to x will vary between -45° and 45° ;
- the rotation angle β with respect to y will vary between 0° and 120° ;
- the rotation angle α with respect to z will vary between 20° and 130° .

Pressure coefficient (C_p) distribution plots obtained from our calculations were very similar

in character for most wing span sections between 25%–75% span. Moreover, only minor changes were observed when the rotation angles β and γ were changed. However, changes of the wing incidence α had considerable effects, as expected. Representative C_p plots obtained for the 50% wing span sections and rotation angles $\beta = 40^\circ$, $\gamma = 0^\circ$ are shown in Figure 5 for $\alpha = 20^\circ$ and $\alpha = 45^\circ$, and for $\alpha = 90^\circ$ and $\alpha = 130^\circ$ in Figure 6. In Figure 6(b) it can be observed that for $\alpha = 130^\circ$ the values of C_p for the upper and lower surfaces changed sign, as compared with the other cases, thus resulting in negative C_L . The corresponding values of the lift coefficient for this case are given in Table 1.

Incidence angle α	Lift coefficient C_L
20°	1.6168
45°	1.0582
90°	0.0422
130°	-1.0033

Table 1 Values of the lift coefficient C_L corresponding to Figure 6(b).

In order to reflect changes in C_L in terms of typical kinematics of insect-like flapping, the quasi-steady values of C_L were associated the appropriate points of time in the flapping cycle, as shown in Figure 7. For this purpose eight values of C_L for varying incidence angle α were used; $C_{L\max} = 2.44$ was obtained for $\alpha = 28.4^\circ$. Variations in the rotation angles β and γ had little effect on the magnitude of C_L with calculations showing differences in the second decimal place.

The values of C_L obtained by the quasi-steady approach are substantially lower than those estimated from those observed in insects for which $C_{L\max}$ of the order of 3 is reported [3]. This underestimate is partially caused by a choice of aerofoil. However, based on the reported aerodynamic experiments [7] and numerical calculations of the hawkmoth *Manduca sexta* [11], it most likely that the effect of a leading edge recirculation vortex has an imperative effect on the flapping wing performance. Hence this phenomenon is associated with unsteady move-

ment of the wing it could not have been investigated by the quasi-steady calculations. In order to provide an in-depth insight into the flapping wing aerodynamics, further work using a time accurate flow solver with dynamically moving wing is necessary.

4 Conclusions

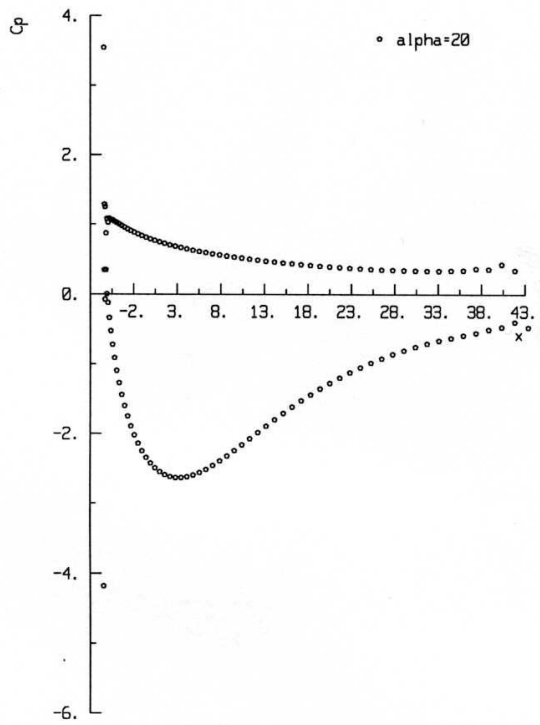
This paper reports the current status of a long-term project investigating aerodynamic aspects of flapping MAVs. The complexities of the physics of the flow have been highlighted and methodologies which could be used to explore it have been defined. An initial quasi-steady numerical model has been developed and applied to an idealised insect-like flapping wing. Although the model provides some initial insight, it is insufficient to capture the important unsteady features of the real flow. A proposed extension of the code should alleviate this problem and is the subject of current work.

Acknowledgement

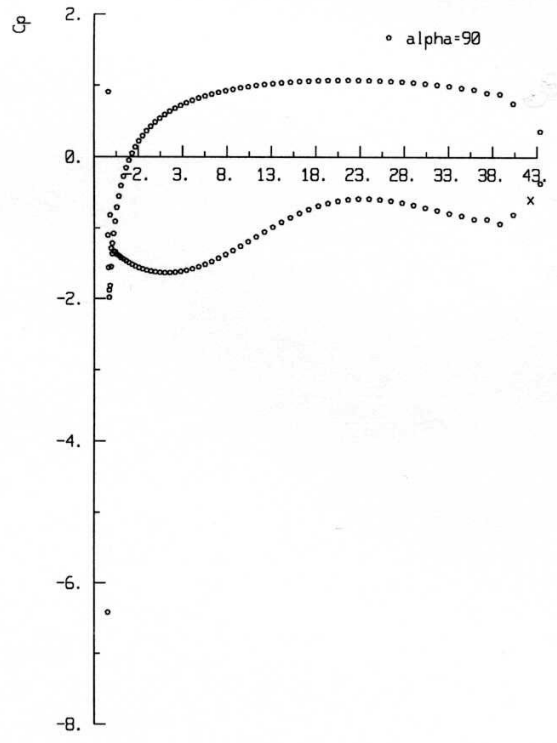
This work has been supported by the EPSRC Grant GR/M78472 “Flapping Flight Aerodynamics of Autonomous Micro Air Vehicles”.

References

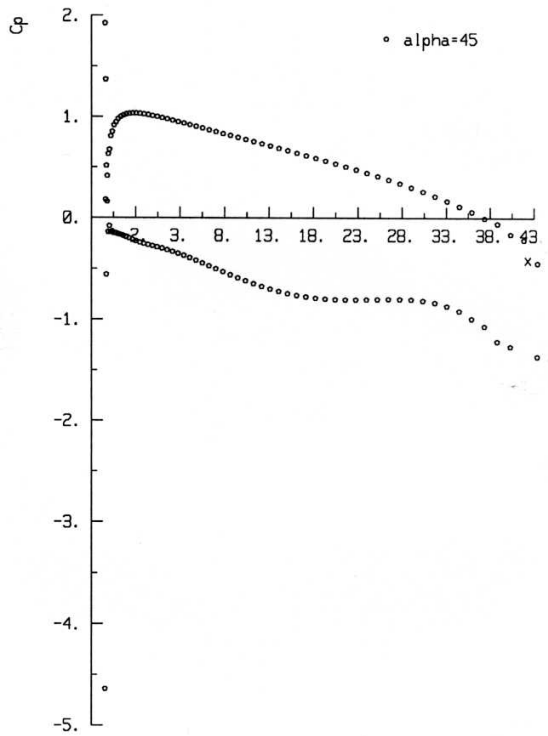
- [1] Adkins C. N and Liebeck R. H. Design of optimum propellers. *J. of Propn & Power*, Vol. 10, No 5, pp 676–682, 1994.
- [2] Chorin A. A numerical method for solving incompressible viscous flow problems. *Journal of Computational Physics*, Vol. 2, pp 12–26, 1967.
- [3] Dickinson M. H, Lehmann F. O, and Sane S. P. Wing rotation and the aerodynamic basis of insect flight. *Science*, Vol. 284, No 5422, pp 1954–1960, 1999.
- [4] Dudley R and Srygley R. B. Flight physiology of neotropical butterflies: Allometry of airspeeds during natural free flight. *Journal of Experimental Biology*, Vol. 191, pp 125–139, 1994.
- [5] Ellington C. P. The aerodynamics of hovering insect flight. VI. Lift and power requirements. *Philosophical Transactions of the Royal Society of London. Series B. Biological Sciences*, Vol. 305, No 1122, pp 145–181, 1984.
- [6] Ellington C. P. Unsteady aerodynamics insect flight. In Ellington C. P and Pedley T. J, editors, *Biological Fluid Dynamics*, Vol. 49, pp 109–129, 1995.
- [7] Ellington C. P, van den Berg C, and Thomas A. P. W. A. L. R. Leading-edge vortices in insect flight. *Nature*, Vol. 384, No 6610, pp 626–630, 1996.
- [8] Farmer J, Martinelli L, and Jameson A. Fast multigrid method for solving incompressible hydrodynamic problems with free surfaces. *AIAA Journal*, Vol. 32, No 6, pp 1175–1182, 1994.
- [9] Gullan P. J and Cranston P. S. *The Insects: An Outline of Entomology*. Chapman & Hall, London, 1994.
- [10] Jameson A. Solution of the Euler equations by a multigrid method. *Applied Mathematics and Computation*, Vol. 13, pp 327–356, 1983.
- [11] Liu H and Kawachi K. A numerical study of insect flight. *Journal of Computational Physics*, Vol. 146, No 1, pp 124–156, 1998.
- [12] Pringle J. W. S. *Insect Flight*. Vol. 52 of *Oxford Biology Readers*, Oxford University Press, Glasgow, 1975.
- [13] Żbikowski R. Flapping wing autonomous micro air vehicles: Research programme outline. *Proc Fourteenth International Conference on Unmanned Air Vehicle Systems*, Vol. [Supplementary Papers], pp 38.1–38.5, 1999.
- [14] Żbikowski R. Flapping wing micro air vehicle: A guided platform for microsensors. *Proc Royal Aeronautical Society Conference on Nanotechnology and Microengineering for Future Guided Weapons*, pp 1.1–1.11, 1999.



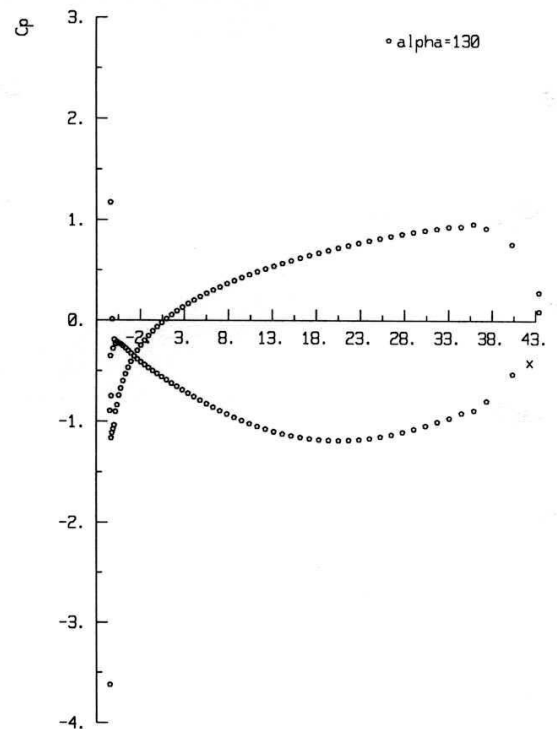
(a)



(a)



(b)



(b)

Fig. 5 Pressure coefficient distribution (C_p) plots for 50% of wingspan for the angles of attack (a) $\alpha = 20^\circ$ and (b) $\alpha = 45^\circ$.

Fig. 6 Pressure coefficient distribution (C_p) plots for 50% of wingspan for the angles of attack (a) $\alpha = 90^\circ$ and (b) $\alpha = 130^\circ$.

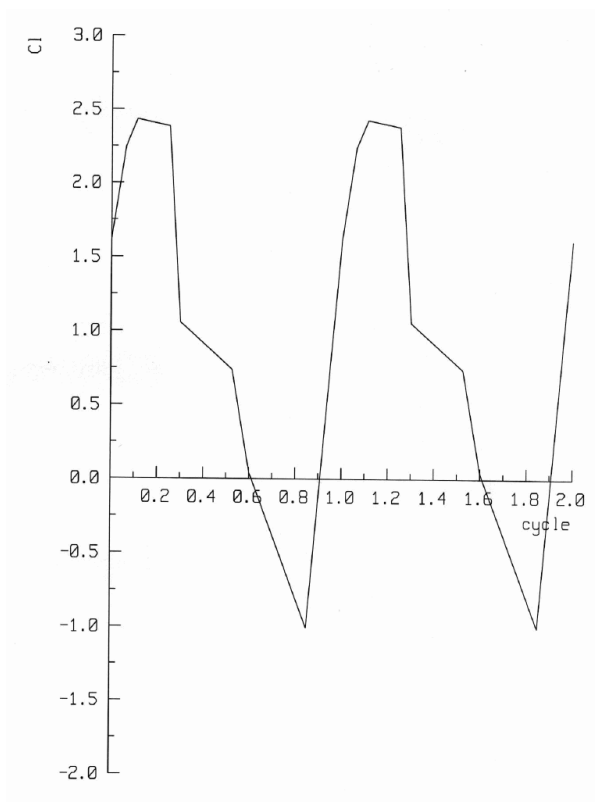


Fig. 7 Variability of the lift coefficient C_L during flapping cycle.